Acta Oceanol. Sin., 2024, Vol. 43, No. 12, P. 102–112
https://doi.org/10.1007/s13131-024-2451-3
http://www.aosocean.com
E-mail: ocean2@hyxb.org.cn

Response of harmful dinoflagellate distribution in the China seas to global climate change

Changyou Wang[1]*, Yuxing Tang[1], Bernd Krock[2], Yiwen Xu[1], Zhuhua Luo[1, 3, 4], Zhaohe Luo[3]*

[1] School of Marine Sciences, Nanjing University of Information Science and Technology, Nanjing 210044, China

[2] Alfred Wegener Institut, Helmholtz Zentrum für Polar– und Meeresforschung, Bremerhaven D–27570, Germany

[3] Third Institute of Oceanography, Ministry of Natural Resources, Xiamen 361005, China

[4] Key Laboratory of Marine Biogenetic Resources, Third Institute of Oceanography, Ministry of Natural Resources, Xiamen 361005, China

Received 21 March 2023; accepted 25 September 2024

Abstract

By establishing a distribution and environmental factor database of 21 typical harmful dinoflagellates in global waters, the MaxEnt model was used to predict shifts in the habitat of harmful dinoflagellates in Chinese waters under global climate change. The results revealed that offshore distance was the most important predictive factor and that surface seawater temperature (SST), primary productivity, and nitrate concentration were the key ecological factors influencing the distribution of harmful dinoflagellates. Under the low greenhouse gas emission scenario defined by the Intergovernmental Panel on Climate Change (IPCC), by approximately 2050, 17 of the 21 harmful dinoflagellate species in high-suitability areas (HSA) will migrate northward, six species will migrate eastward, and six species will expand their HSA. By 2100, approximately 18 of the 21 harmful dinoflagellate species in HSA will have migrated northward, seven species will have migrated eastward, and four species will have expanded their HSA. Notably, the HSA content of highly toxic *Alexandrium minutum* is expected to increase by 13.4% and 9.4% by 2050 and 2100, respectively. Under the high greenhouse gas emissions, there will be 17 species migrating northward, 6 species migrating eastward, and 4 species increasing in their size in HSA by 2050; moreover, there will be 16 species migrating northward, 2 migrating eastward, and 4 species according to their size of HSA by 2100. Specifically, the HSA of *A. minutum* is predicted to increase by 7.0% and 25.9% by 2050 and 2100, respectively. Notably, *A. ostenfeldii*, which is currently seldom present in the China seas, is predicted to exhibit an HSA in most coastal areas of the Yellow Sea, the Bohai Sea, the Hangzhou Bay, the Zhejiang Coast, and the Beibu Gulf of the South China Sea. Conversely, the HSA of *Noctiluca scintillans*, a typical red-tide species, will be reduced by 7%–90%. The northward migration of *Karenia mikimotoi* exceeded 100 km and 300 km under low and high greenhouse gas emission scenarios, respectively. These changes underscore the significant impact of climate change on the distribution and habitat suitability of harmful dinoflagellates, thus indicating a potential shift in their ecological dynamics and consequent effects on marine ecosystems.

Key words: harmful dinoflagellate, climate change, suitable habitat, MaxEnt, species distribution shifts

Citation: Wang Changyou, Tang Yuxing, Krock Bernd, Xu Yiwen, Luo Zhuhua, Luo Zhaohe. 2024. Response of harmful dinoflagellate distribution in the China seas to global climate change. Acta Oceanologica Sinica, 43(12): 102–112, doi: 10.1007/s13131-024-2451-3

1 Introduction

Since the early 20th century, the average surface seawater temperature (SST) worldwide has increased by 0.6℃, causing the distribution range of warm water species to expand towards the poles and the distribution range of cold-water species to shrink (Cai et al., 2020; IPCC, 2019). Since the 1960s, the SST in the China seas has exhibited a significant upward trend. An increasing number of heat waves are occurring as sea levels continue to increase (Cai et al., 2019). In the context of global climate change, the eastern area of China, particularly the East China Sea, is likely to be one of the areas with the greatest future global warming and sea level rise (Cai et al., 2019, 2020; IPCC, 2019, 2021). Harmful algal blooms (HABs) in China predominantly consist of dinoflagellates, with an increasing occurrence of toxic and harmful species (Guo et al., 2014). The unpredictability of these blooms that are significant marine ecological disasters has intensified for coastal stakeholders due to global climate change (Lin et al., 2019; Yu and Chen, 2019; Gu et al., 2022). Therefore, understanding the distribution patterns of harmful dinoflagellates and predicting their future trends can not only provide new theories, technologies, and methods for the prevention and control of harmful dinoflagellate bloom disasters but can also provide scientific support to related industries such as marine fisheries and aquaculture, ultimately reducing economic losses caused by future disasters.

Species distribution models such as Biomod2, MaxEnt, openModeller, and ModEco have been used to analyze the correlation between species distribution data and environmental factors, primarily in the context of terrestrial habitat biogeography (Bertram et al., 2019; Li et al., 2019; Yan et al., 2020).

Foundation item: The National Key Research and Development Program of China under contract Nos 2019YFE0124700 and 2022YFC3106002.

*Corresponding author, E-mail: chywang@nuist.edu.cn; luozhaohe@tio.org.cn

Among these, the MaxEnt model has been extensively employed to predict potential distribution areas of invasive species, identify suitable habitats for endangered and economically important species, and assess species distribution under climate change scenarios (Bertram et al., 2019; Li et al., 2019; Meshgi et al., 2019; Zhang et al., 2019; Yan et al., 2020). Compared to terrestrial species, there are limited reports regarding the use of the MaxEnt model to study the distribution of marine species. Limited data detailing the distribution of marine species are partly responsible for this. Another reason is that planar changes in upper marine habitats are relatively small, and the planar resolution of general marine surveys is low compared with that of terrestrial habitats (Wang et al., 2010; Xie et al., 2019; Melo-Merino et al., 2020). In particular, for global ocean surveys, the grid is above 0.5° in longitude and latitude (http://mds.nmdis.org.cn/).

The MaxEnt model is a species distribution model based on maximum entropy theory (Elith et al., 2011). The maximum entropy principle is a criterion for selecting the probability distribution of random variables that best fits the objective situation (Soofi, 2000). Based on this understanding, it is possible to infer the probability distribution of unknown events from the information of known finite events, as the actual observed real event exhibits the maximum number of approaches to achieve this (Bertram et al., 2019; Li et al., 2019; Meshgi et al., 2019; Yan et al., 2020). The MaxEnt model has been continuously improved and can achieve good prediction results with limited environmental variables and species distribution data (Phillips et al., 2004, 2006, 2017; Phillips and Dudík, 2008). The application of the MaxEnt model to predict species distribution exhibits a small dependence on the sample size of the species distribution data, thus making it suitable for objective situations where there are limited survey data regarding the distribution of harmful dinoflagellates in the ocean (Merow et al., 2013).

Using the MaxEnt model, this study aims to (1) predict the changes in suitable areas for harmful dinoflagellates under global climate change conditions, (2) elucidate the impact of environmental factors such as seawater warming on the potential distribution of harmful dinoflagellates, and (3) discuss new situations faced by marine fisheries, aquaculture, disaster prevention, and reduction.

2 Materials and methods

2.1 *Database development and distribution area division for harmful dinoflagellates*

Using database retrieval (ocean biographic information system, OBIS), literature review (https://www.sciencedirect.com; http://www.springer.com; https://www.cnki.net), and field investigation, we collected information detailing 21 typical, globally distributed harmful dinoflagellate species, including their locations, occurrence times, SST, and salinity, to establish a database of harmful dinoflagellate distribution areas (Table 1). Global ocean assimilation data from the same period were used to supplement missing SST and salinity data for harmful dinoflagellates (China National Marine Science Data Center, 2021).

Referring to the gridding method of the global ocean reanalysis system (China National Marine Science Data Center, 2021), the grids were divided into sizes of 0.5° × 0.5° in terms of longitude and latitude. Longitudes 0°–180°–0° were divided into 720 grids, and latitudes from 75°S to 85°N were divided into 348 grids. Grid sizes gradually change according to 0.4°, 0.3°, 0.25°, 0.25°, 0.3°, and 0.4° between –7.5° and 7.5°. The global oceans were divided into 176 340 distribution blocks, and the distribution areas of the 21 dinoflagellates in the global oceans were counted

Table 1. Number of distribution spots of 21 dinoflagellates in global oceans and the China seas and adjacent waters

	Species	Spots in global oceans	Spots in the China seas and adjacent waters (2°–4°N, 103°–132°E)
1	*Akashiwo sanguinea* (K.Hirasaka) Gert Hansen & Moestrup	7 751	201
2	*Alexandrium minutum* Halim	4 308	4
3	*Alexandrium ostenfeldii* (Paulsen) Balech & Tangen	1 265	1
4	*Azadinium poporum* Tillmann & Elbrächter	96	27
5	*Azadinium spinosum* Elbrächter & Tillmann	274	0
6	*Coolia monotis* Meunier	211	0
7	*Dinophysis acuminata* Claparède & Lachmann	32 775	27
8	*Gambierdiscus toxicus* R.Adachi & Y.Fukuyo	11	0
9	*Gonyaulax spinifera* (Claparède & Lachmann) Diesing	8 635	15
10	*Gonyaulax verior* Sournia	1 167	3
11	*Gymnodinium catenatum* H.W.Graham	1 030	8
12	*Karenia mikimotoi* (Miyake & Kominami ex Oda) Gert Hansen & Moestrup	7 285	280
13	*Karlodinium veneficum* (D.Ballantine) J.Larsen	5 685	4
14	*Lingulodinium polyedra* (F.Stein) J.D.Dodge	9 136	5
15	*Margalefidinium polykrikoides* (Margalef) F.Gómez, Richlen & D.M.Anderson	86	2
16	*Noctiluca scintillans* (Macartney) Kofoid & Swezy	25 959	1 098
17	*Ostreopsis ovata* Y.Fukuyo	30	5
18	*Polykrikos hartmannii* W.M.Zimmermann	262	2
19	*Prorocentrum lima* (Ehrenberg) F.Stein	2 538	152
20	*Protoceratium reticulatum* (Claparède & Lachmann) Bütschli	5 886	30
21	*Pyrodinium bahamense var. compressum* (Böhm) Steidinger, Tester & F.J.R.Taylor	71	40

Note: As some of the collected data detailing harmful dinoflagellate distribution spots were not readily available, this portion of the data was not used to establish a database of harmful dinoflagellate distribution spots. As the database of harmful dinoflagellate distribution areas did not include the appearance time, all collected data regarding harmful dinoflagellate distribution spots were applied when establishing the database of harmful dinoflagellate distribution areas. This resulted in some harmful dinoflagellate species possessing low times and sparse domain frequencies, and this is inconsistent with the data in Tables 1 and 2.

(Table 2). In areas with a high survey frequency, there were numerous records of harmful dinoflagellates, resulting in multiple records in the same distribution area. This makes it possible for survey frequency to affect the prediction results of the model. Therefore, records from the same distribution area were merged to retain only one record from each distribution area.

2.2 *Environmental layer variable selection scheme*

Marine data layers for ecological modeling have attracted the attention of numerous scholars, with over 600 references or applications in related research (http://www.bio-oracle.org). Bio-ORACLE (version 2.2) data provides 18 global geophysical, chemical, biological, and climate data layers with a common spatial resolution (5 arcmin, 9.2 km at the equator) (Tyberghein et al., 2012; Assis et al., 2018). Additionally, we created a data layer for seawater depth and offshore distance based on Natural Earth data at a 1 m:10 m scale (https://www.naturalearthdata.com/) and saved the data in the same format as in Bio-ORACLE version 2.2. The available Bio-ORACLE (version 2.2) for future environmental variables was produced using climate data derived from IPCC predictions (Assis et al., 2018; IPCC, 2019).

Greenhouse gas emission scenarios are the basis for estimating future climate change. The fifth evaluation report of IPCC adopts a new generation scenario termed "Representative Concentration Pathways" (RCPs) (IPCC, 2013). The RCP8.5 scenario (8.5 W/m^2) is the highest greenhouse gas emission scenario. This scenario assumes the largest population, a low technological innovation rate, and slow energy improvement, resulting in slow income growth. This will lead to a long-term high energy demand and high greenhouse gas emissions while lacking policies to address climate change. The RCP2.6 scenario (2.6 W/m^2) is a scenario that limits the global average temperature rise to within 2℃. This scenario was the lowest in terms of greenhouse gas emissions and radiative forcing. From 2010 to 2100, cumulative greenhouse gas emissions will be reduced by 70% compared to those of the baseline year. To achieve this, it is necessary to completely change the energy structure and greenhouse gas emissions other than CO_2 and to promote the use of biomass energy and forest restoration (Shen and Wang, 2013; IPCC, 2019). Based on the current marine data layers for ecological modeling (Bio-ORACLE version 2.2) and combined with future change trends under RCP8.5 and RCP2.6, 50 data layers of environmental variables for 2050 and 2100 were created by overlaying current environmental variables with future increments. These environmental variables consisted of six functions of ten dominant environmental factors, including seawater temperature, salinity, ocean current rate, sea ice thickness, depth, offshore distance, dissolved oxygen, nitrate concentration, phosphate concentration, and primary productivity. The functions include the long-term average of the maximum records per year (suffix Lt.max), the long-term average of the minimum records per year (suffix Lt.min), the long-term average (Suffix Mean), maximum records (Suffix Max), minimum records (Suffix Min), and the range given by the average of the absolute difference between the minimum and maximum records per year (suffix range).

Screening variables that can provide more information to the model and establish a model with good performance using as few variables as possible can improve the adaptability and accuracy of the model predictions (Wang et al., 2023a). The collinearity of environmental variables can exert adverse effects on the modeling process and the interpretation of results (Beaumont, 1981; Wang et al., 2023b; Kariya et al., 2024). To avoid multicollinearity between variables, highly correlated variables were removed, and collinearity analysis was performed for each type of environmental variable. For variables with collinearity, only representative variables were retained, whereas those with collinearity were excluded. A correlation analysis of the 50 related environmental variables was performed using MATLAB 2021. For a group of environmental variables that were significantly correlated at a 0.01 level with a correlation coefficient greater than 0.8 and considering the representativeness and reliability of the data, non-biological environmental variables were preferred, followed by biolo-

Table 2. Number of distribution areas of 21 dinoflagellates in global oceans and the China seas and adjacent waters

	Species	Distribution areas in global oceans	Distribution areas in the China seas and adjacent waters (2°–4°N, 103°–132°E)
1	*Akashiwo sanguinea*	389	25
2	*Alexandrium minutum*	136	5
3	*Alexandrium ostenfeldii*	149	1
4	*Azadinium poporum*	60	6
5	*Azadinium spinosum*	76	0
6	*Coolia monotis*	52	2
7	*Dinophysis acuminata*	1 337	15
8	*Gambierdiscus toxicus*	8	0
9	*Gonyaulax spinifera*	1 124	7
10	*Gonyaulax verior*	112	6
11	*Gymnodinium catenatum*	111	17
12	*Karenia mikimotoi*	148	18
13	*Karlodinium veneficum*	184	6
14	*Lingulodinium polyedra*	360	4
15	*Margalefidinium polykrikoides*	67	23
16	*Noctiluca scintillans*	2 716	76
17	*Ostreopsis ovata*	66	5
18	*Polykrikos hartmannii*	44	12
19	*Prorocentrum lima*	314	12
20	*Protoceratium reticulatum*	467	14
21	*Pyrodinium bahamense var. compressum*	72	19

gical environmental variables. Among the non-biological environmental function variables, the physical environmental variables were preferred, followed by the chemical environmental variables. The dominant environmental variables are presented in Table 3.

Noncollinear variables of the nine selected environmental factors, including ocean current rate, sea ice thickness, temperature, salinity, dissolved oxygen, nitrate, primary productivity, depth, and offshore distance, were used as environmental variables to run the MaxEnt model. The relative contribution and permutation importance of each variable to the predictive ability of the model were calculated (Phillips et al., 2006, 2017; Phillips and Dudík, 2008; Merow et al., 2013), and the importance of environmental factors in regard to the distribution of dinoflagellates was determined based on an analysis of the minimum rank of the relative contribution and permutation importance:

$$\mathrm{EFR}_i = \frac{\sum_{1}^{n}\sum_{j=1}^{6}\min(P_{i1}, ..., P_{ij})}{n},$$

EFR_i, importance rank of i environmental factors on the distribution of dinoflagellates; j, dinoflagellate species; P_{ij}, rank of relative contribution and importance of environmental factors for i environmental factors of j species; n, number of dinoflagellate species.

2.3 *Classification of suitability levels for harmful dinoflagellates and calculation of displacement of suitable areas*

The potential distribution probabilities of the 21 harmful dinoflagellates in the global ocean were calculated using the MaxEnt model, and the distribution probabilities in the China seas and adjacent waters were extracted to construct a distribution map of these harmful dinoflagellates (Supplementary Figures). Based on the IPCC report regarding the classification for likelihood assessment and the actual location of harmful dinoflagellates in the Chinese seas (IPCC, 2019), the level and corresponding range of the suitable area are defined, where a presence probability <0.05 is an unsuitable area, 0.05≤ presence probability <0.33 is a low suitable area, 0.33≤ presence probability <0.66 is a moderate suitable area (MSA), and presence probability ≥0.66 is a high suitable area (HSA).

The average longitude and latitude coordinates of the distribution areas with the same suitability level for harmful dinoflagellates were calculated as the center coordinates of their suitable areas. The differences in the center coordinates between the present suitable area and the future suitable area for harmful dinoflagellates under RCP2.6 and RCP8.5 were defined as the displacement of the suitable area, and the differences in the size between the present HSA and the future HSA under RCP2.6 and RCP8.5 were calculated as the increase (or decrease) in the size of harmful dinoflagellate distribution areas. The average presence probability of harmful dinoflagellate species in the China seas was defined as the arithmetic mean of the presence probabilities of these 21 analyzed harmful dinoflagellate species and was used to quantitatively express the changes in dinoflagellates in a specific distribution area under the background of global change.

3 Results and discussion

3.1 *Changes in suitable area under RCP2.6 Scenario*

Under RCP2.6, by 2050, 17 of the 21 analyzed harmful dinoflagellate species in HSAs will exhibit northward migration compared to their current distributions. Notable exceptions were *Alexandrium ostenfeldii*, *Azadinium spinosum*, *Gonyaulax verior*, and *Margalefidinium polykrikoides* (Table 4). Specifically, *Akashiwo sanguinea*, *Coolia monotis*, *Dinophysis acuminata*,

Table 3. Selected environmental variables for the MaxEnt model of dinoflagellate distribution

	Species	Dominant environmental variable							
		Common	Current velocity	Ice thickness	Nitrate	Salinity	Temperature	Primary productivity 1	Primary productivity 2
1	*Akashiwo sanguinea*	CV.Min Depth.Mean Distance.Mean DO.Range Ice.Min *N*.Range *S*.Range *T*.Range	CV.Range	Ice.Lt.max	*N*.Lt.max	*S*.Min	*T*.Mean	Pr.Max	Pr.Lt.min
2	*Alexandrium minutum*		CV.Range	Ice.Max	*N*.Lt.max	*S*.Min	*T*.Lt.min	Pr.Range	Pr.Lt.min
3	*Alexandrium ostenfeldii*		CV.Range	Ice.Max	*N*.Mean	*S*.Min	*T*.Mean	Pr.Range	Pr.Min
4	*Azadinium poporum*		CV.Mean	Ice.Max	*N*.Lt.max	*S*.Lt.min	*T*.Min	Pr.Range	Pr.Lt.min
5	*Azadinium spinosum*		CV.Lt.max	Ice.Max	*N*.Lt.max	*S*.Min	*T*.Mean	Pr.Range	Pr.Lt.min
6	*Coolia monotis*		CV.Mean	Ice.Max	*N*.Lt.min	*S*.Lt.min	*T*.Min	Pr.Range	Pr.Lt.min
7	*Dinophysis acuminata*		CV.Max	Ice.Range	*N*.Mean	*S*.Max	*T*.Mean	Pr.Range	Pr.Lt.min
8	*Gambierdiscus toxicus*		CV.Max	Ice.Max	*N*.Min	*S*.Min	*T*.Min	Pr.Lt.max	Pr.Lt.min
9	*Gonyaulax spinifera*		CV.Lt.max	Ice.Range	*N*.Lt.min	*S*.Min	*T*.Max	Pr.Range	Pr.Lt.min
10	*Gonyaulax verior*		CV.Range	Ice.Lt.max	*N*.Lt.min	*S*.Lt.max	*T*.Max	Pr.Max	Pr.Lt.min
11	*Gymnodinium catenatum*		CV.Lt.max	Ice.Lt.max	*N*.Mean	*S*.Min	*T*.Lt.min	Pr.Range	Pr.Min
12	*Karenia mikimotoi*		CV.Lt.max	Ice.Max	*N*.Lt.min	*S*.Mean	*T*.Mean	Pr.Lt.max	Pr.Lt.min
13	*Karlodinium veneficum*		CV.Lt.max	Ice.Range	*N*.Lt.min	*S*.Max	*T*.Max	Pr.Lt.max	Pr.Min
14	*Lingulodinium polyedra*		CV.Lt.max	Ice.Lt.max	*N*.Max	*S*.Min	*T*.Mean	Pr.Max	Pr.Min
15	*Margalefidinium polykrikoides*		CV.Range	Ice.Lt.max	*N*.Mean	*S*.Lt.min	*T*.Max	Pr.Max	Pr.Min
16	*Noctiluca scintillans*		CV.Range	Ice.Max	*N*.Lt.min	*S*.Min	*T*.Lt.min	Pr.Max	Pr.Lt.min
17	*Ostreopsis ovata*		CV.Lt.max	Ice.Max	*N*.Lt.max	*S*.Lt.min	*T*.Mean	Pr.Range	Pr.Min
18	*Polykrikos hartmannii*		CV.Mean	Ice.Lt.max	*N*.Mean	*S*.Min	*T*.Lt.min	Pr.Range	Pr.Lt.min
19	*Prorocentrum lima*		CV.Lt.max	Ice.Lt.max	*N*.Lt.max	*S*.Lt.min	*T*.Lt.min	Pr.Range	Pr.Lt.min
20	*Protoceratium reticulatum*		CV.Lt.max	Ice.Range	*N*.Lt.min	*S*.Lt.min	*T*.Mean	Pr.Max	Pr.Min
21	*Pyrodinium bahamense var. compressum*		CV.Lt.max	Ice.Max	*N*.Min	*S*.Min	*T*.Min	Pr.Lt.max	Pr.Lt.min

Note: CV represents current velocity; Ice represents ice thickness; DO represents dissolved oxygen; *N* represents nitrate concentration; *S* represents salinity; *T* represents temperature; Pr represents primary productivity.

Table 4. Number of changes in the suitable habitat for 21 typical harmful dinoflagellates

Year	Scenario	Number of dinoflagellates								
		Low suitable area			Moderate suitable area			High suitable area		
		D_N/km	D_E/km	V_S/%	D_N/km	D_E/km	V_S/%	D_N/km	D_E/km	V_S/%
2050	RCP2.6	16	3	2	16	6	4	17	6	6
	RCP8.5	17	4	2	16	4	3	17	6	4
2100	RCP2.6	15	5	3	16	8	4	18	7	4
	RCP8.5	17	2	2	16	4	2	16	2	4

Note: D_N, the distance moved northward; D_E, the distance moved eastward; V_S, size increased by.

Gonyaulax spinifera, *Gymnodinium catenatum*, *Karenia mikimotoi*, *Karlodinium veneficum*, *Lingulodinium polyedra*, *Noctiluca scintillans*, *Ostreopsis ovata*, and *Prorocentrum lima* that have moved northward for over 100 km, reaching 245.9 km, 174.1 km, 147.7 km, 433.0 km, 173.1 km, 102.3 km, 130.4 km, 486.3 km, 182.3 km, 360.3 km, and 178.5 km, respectively (Table 5). In addition to the northward migration, several species displayed eastward movement within their HASs, albeit to a lesser extent. Among these, *A. sanguinea* exhibited the greatest eastward migration, exceeding 50 km. Other species with notable eastward shifts included *A. ostenfeldii*, *C. monotis*, *M. polykrikoides*, *N. scintillans*, and *Polykrikos hartmannii*. Furthermore, six species exhibited an increase in HSA size (Table 4). *Alexandrium minutum*, *A. ostenfeldii*, *A. spinosum*, *C. monotis*, *P. lima*, and *Protoceratium reticulatum* increased by 13.4%, 13.6%, 8.5%, 0.05%, 0.17%, and 0.64%, respectively.

Currently, *A. ostenfeldii*, *A. spinosum*, and *Gambierdiscus toxicus* are limited to the China seas and adjacent waters (Gu et al., 2013; Xu et al., 2021). However, under RCP2.6 in 2050, *A. ostenfeldii* is expected to receive HSAs in most coastal areas of the Yellow Sea and on the northern and southern coasts of the Bohai Sea, Hangzhou Bay, Zhejiang Province, and Beibu Gulf of the South China Sea (Fig. S1c). *Azadinium spinosum* is projected to receive HSAs along the northern coast of the Bohai Sea, the northern and eastern coasts of the Yellow Sea, the eastern East China Sea, and the Beibu Gulf of the South China Sea (Fig. S1e). *Gambierdiscus toxicus* is expected to receive HSAs in most of the South China Sea and the eastern East China Sea (Fig. S1h). Under RCP2.6 2050, the size of areas of high suitability for *A. sanguinea* in the China seas will decrease by approximately 28.6% and will only be distributed along the coast of Beibu Gulf and the Taiwan Strait, with smaller patches along the eastern and southern coasts of the Korean Peninsula (Fig. S1a). *Gonyaulax verior* is currently present in the Bohai Sea, Yellow Sea, and South China Sea, but the China seas and adjacent waters will become unsuitable habitats by 2050 under RCP2.6 (Fig. S1j). *Polykrikos hartmanii* is also not expected to receive HSA in the China seas under RCP2.6 in 2050 (Fig. S1r). Significant reductions in HSA size have been reported in several species, including *Azadinium poporum*, *D. acuminata*, *G. toxicus*, *G. spinifera*, *G. catenatum*, *K. mikimotoi*, *K. veneficum*, *L. polyedra*, *M. polykrikoides*, *N. scintillans*, *O. ovata*, *P. hartmanii*, and *Pyrodinium bahamense* var. *compressibum*, with decreases ranging from 6.6% to 80% (Figs S1d, f–i, k–r, and u).

Table 5. Changes in the habitat of 21 typical harmful dinoflagellates

	Species	HSA at present/ km²	RCP2.6						RCP8.5					
			2050			2100			2050			2100		
			D_N/km	D_E/km	V_S/%	D_N/km	D_E/km	V_S/%	D_N/km	D_E/km	V_S/%	D_N/km	D_E/km	V_S/%
1	*Akashiwo sanguinea*	200 209.6	245.9	72.3	–28.6	231.2	68.8	–26.5	323.1	54.6	–29.8	762.9	–199.2	–63.4
2	*Alexandrium minutum*	67 571.9	30.7	–6.7	13.4	30.9	–4.7	9.4	59.5	–21.8	7.0	166.9	–49.4	25.9
3	*Alexandrium ostenfeldii*	216 556.8	–2.1	17.2	13.6	6.6	14.7	7.3	22.8	10.1	3.3	145.0	–24.5	12.1
4	*Azadinium poporum*	41 364.8	4.6	–13.2	–6.6	30.5	–16.5	–8.0	7.6	–18.5	–14.8	34.6	–41.7	–36.8
5	*Azadinium spinosum*	619 102.0	–34.2	–17.0	8.5	–33.7	–5.1	3.8	–20.4	–20.8	11.3	–42.3	–46.7	16.9
6	*Coolia monotis*	69 597.8	174.1	24.7	0.1	159.8	11.4	–8.2	173.2	19.1	0.3	427.2	72.0	24.5
7	*Dinophysis acuminata*	914 189.6	147.7	–12.4	–2.9	131.0	–6.7	–4.7	170.0	–17.1	–4.1	302.4	–82.9	–13.9
8	*Gambierdiscus toxicus*	1 723 326.5	61.3	–47.5	–31.6	52.2	–22.2	–25.6	28.8	–81.6	–41.8	14.4	–89.2	–47.1
9	*Gonyaulax spinifera*	584 764.3	433.0	–51.3	–47.4	375.3	–55.8	–37.3	815.9	–110.2	–64.3	1 254.0	–306.5	–94.5
10	*Gonyaulax verior*	0.0	0.0	0.0	0.0	0.0	0.0	0.0	0.0	0.0	0.0	0.0	0.0	0.0
11	*Gymnodinium catenatum*	189 890.6	173.1	–72.8	–24.6	138.5	–59.5	–25.4	160.2	–67.2	–22.4	385.4	–159.0	–46.5
12	*Karenia mikimotoi*	139 071.7	102.3	–66.3	–23.0	74.3	–55.0	–22.6	128.9	–70.9	–25.7	325.0	–117.4	–59.8
13	*Karlodinium veneficum*	370 537.3	130.4	–8.9	–14.0	99.6	–7.9	–14.7	217.2	–1.1	–22.8	371.0	–101.8	–28.7
14	*Lingulodinium polyedra*	808 766.7	486.3	–29.1	–30.2	457.6	–19.6	–27.2	551.7	–45.3	–34.0	750.3	–102.4	–48.4
15	*Margalefidinium polykrikoides*	227 992.4	–270.1	15.0	–21.2	–195.0	6.5	–14.7	–246.6	3.5	–28.3	–410.1	–1.1	–49.3
16	*Noctiluca scintillans*	1 600 532.5	182.3	32.3	–13.7	132.7	36.9	–6.7	283.1	8.7	–19.8	571.8	–86.1	–30.6
17	*Ostreopsis ovata*	6 608.2	360.3	–28.9	–79.9	254.2	–31.9	–78.6	601.5	–289.9	–89.5	–	–	–100.0
18	*Polykrikos hartmannii*	28 540.8	1.7	0.1	–29.9	27.6	10.8	–20.4	–13.3	19.9	–39.8	–85.9	31.5	–55.1
19	*Prorocentrum lima*	738 403.0	178.5	–2.9	0.2	166.0	–8.1	–0.7	187.0	–1.4	–1.6	351.4	–36.0	–8.5
20	*Protoceratium reticulatum*	581 481.4	14.9	–3.8	0.6	7.1	–1.3	0.003	35.6	–9.5	–2.2	100.8	–43.2	–13.0
21	*Pyrodinium bahamense* var. *compressum*	96 582.8	60.9	–8.7	–19.3	46.5	6.2	–13.3	92.9	–20.2	–35.9	150.6	–104.7	–59.5

Note: HSA represents highly suitable area; D_N represents the distance moved northward; D_E represents the distance moved eastward; V_S represents size increased by; RCP represents representative concentration pathway.

A total of 18 out of 21 harmful dinoflagellate species in HSAs are predicted to migrate northward under RCP2.6 in 2010 compared to the present ones, with the exceptions of *A. spinosum*, *G. verior*, and *M. polykrikoides* (Table 4). In particular, *A. sanguinea*, *C. monotis*, *D. acuminata*, *G. spinifera*, *G. catenatum*, *L. polyedra*, *N. scintillans*, *O. ovata*, and *P. lima* are anticipated to move northward by over 100 km, ultimately reaching 231.2 km, 159.8 km, 131.0 km, 375.3 km, 138.5 km, 457.6 km, 132.7 km, 254.2 km, and 166.0 km, respectively (Table 5). An eastward migration was also expected for *A. sanguinea*, *A. ostenfeldii*, *C. monotis*, *M. polykrikoides*, *N. scintillans*, *P. hartmannii*, and *Pyrodinium bahamense* var. *compressum*, although predominantly in *A. sanguinea*, which is predicted to move more than 50 km eastward. Additionally, four species, including *A. minutum*, *A. ostenfeldii, A. spinosum*, and *P. reticulatum*, increased the size of HSAs by 9.4%, 7.3%, 3.8%, and 0.003%, respectively (Table 5). Compared to that predicted in 2050, the size of *A. sanguinea* in the HSAs of the China seas will have expanded from 140 000 km^2 to 150 000 km^2 in 2100 and is mainly distributed along the coast of the Beibu Gulf, the Taiwan Strait, and the coast of the Korean Peninsula (Fig. S2a). The HSAs of *A. ostenfeldii* are mainly distributed along the northern and southern coasts of the Bohai Sea, the eastern and western coasts of the Yellow Sea, Hangzhou Bay, and the coast of Zhejiang Province, but they have been reduced in size in the Yellow Sea compared to the present size. There were also sporadic HSAs of *A. ostenfeldii* along the coast of Beibu Gulf in the South China Sea (Fig. S2c). *Azadinium spinosum* exhibits large HSAs along the eastern coast of the Yellow Sea, the eastern East China Sea, and the Beibu Gulf of the South China Sea; however, several small HSAs occur along the coast of the Shandong Peninsula. Compared with that predicted for 2050, the size of *A. spinosum* is expected to decrease by 2100 (Fig. S2e). Similar to the prediction for 2050, *G. verior* will not exhibit HSAs in the China seas or adjacent waters (Fig. S2j) in 2100, nor will *P. hartmanii* in the China seas (Fig. S2r). However, *G. toxicus* possesses areas of high suitability in the South China sea and East China sea (Fig. S2h).

The HSA sizes of *A. sanguinea*, *A. poporum*, *C. monotis*, *D. acuminata*, *G. toxicus*, *G. spinifera*, *G. catenatum*, *K. mikimotoi*, *K. veneficum*, *L. polyedra*, *M. polykrikoides*, *N. scintillans*, *O. ovata*, *P. hartmanii*, *P. lima*, and *Pyrodinium bahamense var. compressibum* will exhibit a decrease of 4.7% to 78.6% by 2100 (Figs 2a, d, f–i, k–s, u) compared to the present ranges.

As a whole, under the RCP2.6, the overall suitable area, an average presence probability of all 21 analyzed harmful dinoflagellate species is ⩾0.33, and they will move northward for over 240 km and 226 km by 2050 and 2100, respectively, compared to their current area. The overall suitable area is expected to decrease by 19.1% and 16.4% by 2050 and 2100, respectively. However, the meridional migration distance of the total HSA was <15 km (Fig. 1).

3.2 *Changes in suitable area under RCP8.5 Scenario*

In 2050, 17 of the 21 harmful dinoflagellate species in HSAs will migrate northward under RCP8.5 compared to the present values, with the exception of *A. spinosum*, *G. verior*, *M. polykrikoides,* and *P. hartmannii*. In particular, *A. sanguinea*, *C. monotis*, *D. acuminata*, *G. catenatum*, *N. scintillans*, and *P. lima* moved northward by over 100 km. *Lingulodinium polyedra* moved over 500 km, *O. ovata* moved over 600 km, and *G. spinifera* moved over 800 km, respectively (Table 5). Moreover, *A. sanguinea*, *A. ostenfeldii*, *C. monotis*, *M. polykrikoides*, *N. scintillans*, and *P. hartmannii* migrated eastward in highly suitable areas, although the eastward migration distance was relatively small. Only *A. sanguinea* moved eastward over 50 km. Only 4 of the 21 harmful dinoflagellate species (*A. minutum*, *A. ostenfeldii*, *A. spinosum*, and *C. monotis*) increased in size by 7.0%, 3.3%, 11.3%, and 0.3%, respectively (Table 5). Similar to RCP2.6 2050, *G. verior* and *P. hartmanii* did not receive HSAs in the China seas (Figs S3j, r). *Dinophysis acuminata* causes HSAs along the entire coast of the China seas, but its distribution area has decreased by 4.1% compared to the present distribution. The HSA sizes of *A. sanguinea*, *A. poporum*, *D. acuminata*, *G. toxicus*, *G. spinifera*, *G. catenatum*, *K. mikimotoi*, *K. veneficum*, *L. polyedra*, *M. polykrikoides*, *N. scintillans*, *O. ovata*, *P. hartmanii*, *P. lima*, *P. reticulatum*, and *Pyrodinium bahamense* var. *compressibum* decreased by 29.8% on average, ranging from 1.6% to 89.5% (Table 5) (Figs S3a, d, g–i, k–u).

Under RCP8.5 as projected for 2100, the HSAs of 16 of the 21 harmful dinoflagellate species will shift northward compared to their current positions, with the exception of *A. spinosum*, *G. verior*, *M. polykrikoides*, *O. ovata*, and *P. hartmannii*. Particularly, *A. minutum*, *A. ostenfeldii*, *C. monotis*, *D. acuminata*, *G. catenatum*, *K. mikimotoi*, *K. veneficum*, *P. lima*, *P. reticulatum*, and *Pyrodinium bahamense* var. *compressibum* are predicted to move northward by over 100 km. *Noctiluca scintillans* moved over 500 km, *A. sanguinea* and *L. polyedra* moved over 600 km, and *G. spinifera* moved over 1 200 km (Table 5). Moreover, *C. monotis* and *P. hartmannii* migrated eastward in highly suitable areas, although their eastward migration distances were relatively small. Only *C. monotis* moved more than 50 km eastward. Additionally, four species (*A. minutum*, *A. ostenfeldii*, *A. spinosum*, and *C. monotis*) exhibited an increase in the size of HSA by 25.9%, 12.1%, 16.9%, and 24.5%, respectively. *Gonyaulax verior*, *O. ovata*, and *P. hartmanii* did not produce HSAs in the China seas (Figs S4j, q and r).

The sizes of *A. sanguinea*, *A. poporum*, *D. acuminata*, *G. toxicus*, *G. spinifera*, *G. catenatum*, *K. mikimotoi*, *K. veneficum*, *L. polyedra*, *M. polykrikoides*, *N. scintillans*, *P. hartmanii*, *P. lima*, *P. reticulatum*, and *Pyrodinium bahamense* var. *compressibum* were predicted to decrease significantly, ranging from 8.5% to 94.5%, by 2100 (Table 5) (Figs S4a, d, g–i, k–p, r–u).

Under RCP8.5, the overall suitable area will move northward by over 265 km and 535 km by 2050 and 2100, respectively, compared to the current area. The overall suitable area is expected to decrease by 22.7% and 42.9% by 2050 and 2100, respectively. However, the overall suitable area will move westward by 26 km by 2050 and 150 km by 2100 (Fig. 1).

3.3 *Impact of global changes on the habitat of harmful dinoflagellates*

Although 15 variables consisting of nine environmental factors were used in the MaxEnt model for each species (Table 3), five of them contributed to an average of 85% (ranging from 71% to 97%) of the predictive power of the model (Table 6). Therefore, this discussion focused on the five most influential environmental factors.

According to the EFR calculated using the relative contribution and permutation importance of each environmental variable (Phillips and Dudík, 2008; Phillips et al., 2017; Merow et al., 2013), offshore distance was the most important predictive factor and ranked among the top five most important environmental factors for all 21 dinoflagellate species, with 12 species ranking first (Table 7). Seawater depth was ranked among the five most important environmental factors for 19 species, with seven species ranking first. This indicates that the 21 dinoflagellate species primarily belong to nearshore environments (Qi et al., 2003; Lin

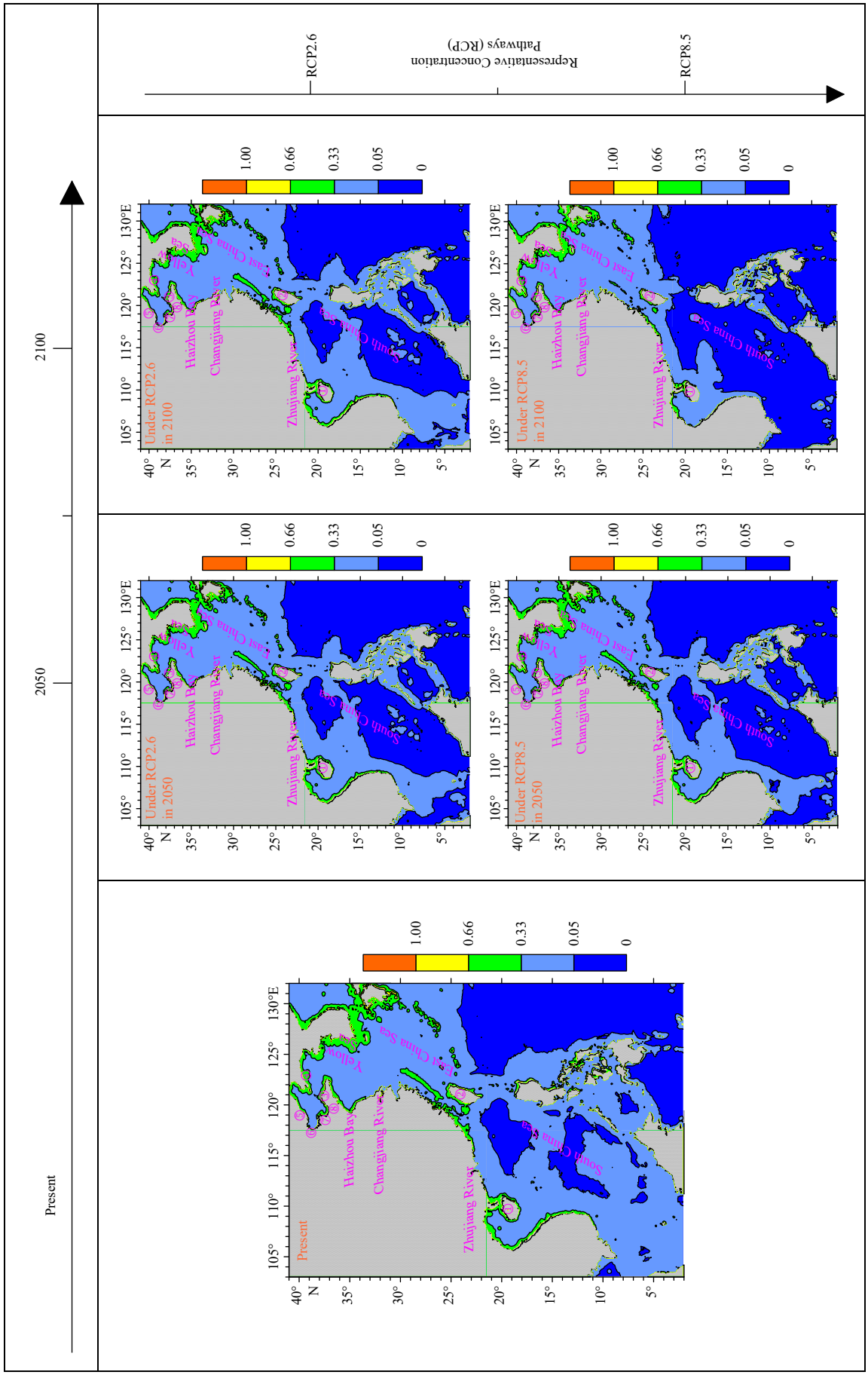

Fig. 1. The average value of cloglog of 21 dinoflagellates in the China seas and adjacent waters currently (left), under RCP2.6 (middle up) and RCP8.5 (middle down) in 2050, and under RCP2.6 (right up) and RCP8.5 (right down) in 2100 (number symbol ①: Hainan Island; ②: Taiwan Island; ③: Shandong Peninsula; ④: Changshan Archipelago; ⑤: Zhimao Bay; ⑥: Bohai Bay; ⑦: Laizhou Bay; ⑧: Jiaozhou Bay; ⑨: Beibu Gulf) (color bar, blue: unsuitable area; baby blue: low suitable area; green: moderate suitable area; yellow: high suitable area; orange: high suitable area with a presence probability of 1).

Table 6. Rank of environmental function variables impacts on the distribution of species of dinoflagellates

	Species	ST5/%	Environmental factors rank				
			1	2	3	4	5
1	*Akashiwo sanguinea*	84	Distance.Mean	Depth.Mean	Nitrate.Lt.max	Primary. productivity.Lt.min	Temperature.Mean
2	*Alexandrium minutum*	85	Depth.Mean	Distance.Mean	Primary. productivity.Lt.min	Temperature.Lt.min	Dissolved.oxygen. Range
3	*Alexandrium ostenfeldii*	83	Depth.Mean	Nitrate.Mean	Distance.Mean	Dissolved.oxygen.Range	Temperature.Mean
4	*Azadinium poporum*	85	Depth.Mean	Primary. productivity.Lt.min	Distance.Mean	Nitrate.Range	Temperature.Min
5	*Azadinium spinosum*	79	Primary. productivity.Lt.min	Depth.Mean	Distance.Mean	Dissolved.oxygen.Range	Nitrate.Range
6	*Coolia monotis*	92	Distance.Mean	Depth.Mean	Temperature.Range	Ice.thickness.Max	Primary. productivity.Lt.min
7	*Dinophysis acuminata*	84	Distance.Mean	Depth.Mean	Nitrate.Mean	Temperature.Mean	Primary. productivity.Lt.min
8	*Gambierdiscus toxicus*	97	Distance.Mean	Nitrate.Min	Temperature.Min	Salinity.Range	Ice.thickness.Max
9	*Gonyaulax spinifera*	71	Distance.Mean	Depth.Mean	Dissolved.oxygen. Range	Temperature.Max	Primary. productivity.Lt.min
10	*Gonyaulax verior*	87	Depth.Mean	Distance.Mean	Temperature.Max	Primary. productivity.Lt.min	Salinity.Range
11	*Gymnodinium catenatum*	86	Distance.Mean	Depth.Mean	Temperature.Lt.min	Ice.thickness.Lt.max	Temperature.Range
12	*Karenia mikimotoi*	88	Temperature.Mean	Depth.Mean	Primary. productivity.Lt.min	Distance.Mean	Nitrate.Lt.min
13	*Karlodinium veneficum*	84	Depth.Mean	Distance.Mean	Salinity.Range	Current.Velocity.Lt.max	Dissolved.oxygen. Range
14	*Lingulodinium polyedra*	77	Distance.Mean	Temperature.Mean	Primary. productivity.Min	Temperature.Range	Depth.Mean
15	*Margalefidinium polykrikoides*	84	Depth.Mean	Distance.Mean	Ice.thickness.Min	Ice.thickness.Lt.max	Salinity.Range
16	*Noctiluca scintillans*	88	Distance.Mean	Primary. productivity.Lt.min	Temperature.Lt.min	Salinity.Min	Depth.Mean
17	*Ostreopsis ovata*	91	Distance.Mean	Temperature.Mean	Ice.thickness.Max	Temperature.Range	Current.Velocity. Lt.max
18	*Polykrikos hartmannii*	86	Distance.Mean	Depth.Mean	Temperature.Lt.min	Primary. productivity.Range	Temperature.Range
19	*Prorocentrum lima*	87	Distance.Mean	Primary. productivity.Lt.min	Depth.Mean	Temperature.Lt.min	Primary. productivity.Range
20	*Protoceratium reticulatum*	79	Depth.Mean	Temperature.Mean	Dissolved.oxygen. Range	Distance.Mean	Temperature.Range
21	*Pyrodinium bahamense* var. *compressum*	94	Distance.Mean	Temperature.Min	Current.Velocity. Lt.max	Depth.Mean	Temperature.Range

Note: ST5 represents sum of the top five environmental variables contributing to the model's predictive ability.

Table 7. Importance rank of environmental factors on the distribution of dinoflagellates

	Environmental factors								
	Spatial variable		Ecological factor						
	Distance	Depth	Temperature	Primary productivity	Nitrate	Ice thickness	Dissolved oxygen	Salinity	Current velocity
EFR	1.8	2.1	3.2	3.3	3.4	3.8	4.0	4.2	4.0
n	21	19	18	13	7	5	6	5	3

Note: EFR represents importance rank of environmental factors on the distribution of dinoflagellates; *n* represents number of species among the 21 typical dinoflagellate species.

et al., 2019), which is consistent with the importance of altitude in terrestrial habitats (Wang et al., 2017). Spatial variables in the ocean, such as seawater depth and offshore distance, also strongly influenced the distribution of harmful dinoflagellates in seawater (Table 6). Only *A. sanguinea* and *C. monotis* will move more than 50 km eastward and will not move more than 100 km. This was irrespective of RCP2.6 or 8.5 (Table 5), indicating that the behavior of nearshore species did not change.

Surface seawater temperature (SST) has emerged as a critical ecological factor, ranking among the top five most important environmental factors for 18 dinoflagellates, with *K. mikimotoi* ranking first. *Karenia mikimotoi* exhibits the second largest cumulative area of harmful algal blooms (HABs), possibly being the most important HAB species in China in terms of the economic losses (Liu et al., 2015; Lü et al., 2019; Gu et al., 2022; Ministry of Natural Resources of the People's Republic of China, 1998–2022). The rise in SST would promote the northward migration of *K. mikimotoi* more than 100 km and 300 km under RCP 2.6 and 8.5, respectively (Table 5). This will likely lead to *K. mikimotoi* becoming a common species in the Yellow Sea and increase the risk of developing HAB (Wang et al., 2024). Furthermore, SST ranked among the top ecological factors for 11 dinoflagellate species: *C. monotis*, *G. toxicus*, *G. verior*, *G. catenatum*, *L. polyedra*, *N. scintillans*, *O. ovata*, *P. hartmannii*, *P. reticulatum*, and *Pyrodinium bahamense* var. *compressum*, indicating that changes in temperature have a significant effect on their distribution. Interestingly, the contribution of offshore distance to the prediction of dinoflagellate distribution was greater than that of temperature (Table 7), as the studied dinoflagellates were primarily nearshore species, and temperature changes were not as significant as offshore dis-

tance changes.

Primary productivity was the second most important ecological factor and ranked among the five most important environmental factors for the 13 dinoflagellate species, with *A. spinosum* ranking first. Although *A. spinosum* has not been documented in the China seas as a *de novo* producer of azaspiracids (Tillmann et al., 2009), it is currently larger than 619 100 km^2 with an average increase of 10% under global climate change (Table 5). Their potential expansion poses a significant risk to marine fisheries and aquaculture systems. Cysts of *A. spinosum* have been identified along the coast of the China seas (Wang et al., 2022). Moreover, primary productivity ranks among the top 1 in the ecological factors for seven dinoflagellates, *A. minutum, A. poporum, Karenia mikimotoi, L. polyedra, N. scintillans,* and *P. lima*, indicating great potential for the expansion of these heterotrophic or mixotrophic species, with further increases in primary productivity and eutrophication levels in the China seas and adjacent waters (Burkholder et al., 2008).

Nitrate concentration was the third most important ecological factor and ranked among the top five most important environmental factors for seven dinoflagellate species, with no species ranking first. However, nitrate concentration was ranked among the top ecological factors for the four dinoflagellate species, *A. sanguinea*, *A. ostenfeldii*, *D. acuminata*, and *G. toxicus* (Table 7). This indicates that aggravated eutrophication is beneficial for the diffusion of these autotrophic and mixotrophic species and could even trigger blooms in the China seas and adjacent waters (Burkholder et al., 2008; Wang et al., 2024). *Akashirvo sanguinea* has frequently bloomed in Chinese waters since 1998 and has been categorized as a species that causes irregular blooms (Chen et al., 2019). *Alexandrium ostenfeldii*, occurring usually in coastal areas at high latitudes, was reported to be present in the China seas in 2011 (Gu, 2011). *Akashirvo sanguinea*, *D. acuminata*, and *G. toxicus* are examples of free-living, mixotrophic, and harmful algal species that thrive in eutrophic estuarine marine coastal waters (Burkholder et al., 2008; Chen et al., 2019). These records partially support the importance of nutrients for dinoflagellate species during autotrophy and mixotrophy.

Ice thickness was ranked among the top ecological factors for *M. polykrikoides* and *O. ovata*, dissolved oxygen for *G. spinifera* and *P. reticulatum*, salinity for *K. veneficum*, and ocean current velocity for *P. bahamense* var. *compressum* ranked among the top ecological factors for these organisms.

According to the IPCC Assessment Report (IPCC, 2021), the increases in temperature are an important projection of global climate change, and global mean SST would increase by 0.64–0.73℃ with a range from 0.20℃ to 1.27℃ under RCP2.6 from 2050 to 2100. The projected change would be up to 0.95–2.58℃ with a range from 0.60℃ to 3.51℃ under RCP8.5 from 2050 to 2100 (IPCC, 2019). An increase in SST will significantly affect biodiversity and adaptability (IPCC, 2019; Cai et al., 2020). As presented in Table 5, more than 70%–80% of the species would suffer a decrease in HSA in the near term (2050) and at the end of the century (2100) relative to current levels. Some species, such as *Osteopsis ovata*, have completely lost their HSA in the China seas, posing a significant threat to biodiversity. Conversely, although *A. ostenfeldii*, *A. spinosum,* and *G. toxicus* rarely occur in the China seas and adjacent waters, they possess a suitable area with a current size of more than 2.2×10^5 km^2 regardless of the RCP (Figs S1–4), indicating an increase in their adaptability. Nevertheless, HSA for *G. verior* is lacking in the China seas, both currently and in the future, regardless of the RCP.

The northward migration of 70%–80% of dinoflagellate species poses a serious challenge to China, possibly resulting in the emergence of new types of HABs in the northern China seas (Gu et al., 2022). HABs in China have primarily occurred in the Bohai Sea and southeastern coastal waters of the China seas over the past 30 years (Zhang, 2013; Guo et al., 2015); however, the frequency and area of HABs caused by dinoflagellates in the Yellow Sea have increased in recent years (Ministry of Natural Resources of the People's Republic of China, 1998–2022; Wang et al., 2023a). In particular, as one of the top disasters caused by dinoflagellate blooms in China, *N. scintillans* exhibit the highest frequency of HABs as dominant organisms in recent years, while the *K. mikimotoi* and *G. catenatum* exert the most serious effects of HABs caused by toxic species on social life and production (Gu et al., 2013; Lü et al., 2019; Li, 2021; Ministry of Natural Resources of the People's Republic of China, 1998–2022; Wang et al., 2023a). A previous study reported that 173 species of HAB organisms could produce toxins or exert toxic effects (http://www.marinspecies.org/hab), 94 of which are dinoflagellates (Lin et al., 2019). The northward migration of harmful dinoflagellates affects the primary productivity and ecosystem structure in the China seas and adjacent waters. Therefore, more attention should be paid to the future biogeographical impacts of climate change on toxin-producing species and to proactive response measures. Although suggestions for improving the information level in HAB monitoring, risk assessment, and graded HABs forecasting have been proposed based on the characteristics of HAB disasters along the coast of the China seas (Guo et al., 2014; Zhou et al., 2020), the environmental management of coastal habitats and ecosystems in relation to marine fisheries and aquaculture should be studied further.

4 Conclusions

Based on the calculation of the EFR for the distribution of dinoflagellates, offshore distance was observed to be the most important predictive factor for detecting HSA (similar to the altitude of terrestrial habitats), and this is an important environmental variable affecting species distribution. SST was the most important ecological factor and ranked among the top ecological factors for 11 out of 21 species and led to the northward migration of 14 species, particularly toxic species such as *K. mikimotoi* and *G. catenatum*. This poses a serious challenge for the environmental management of coastal habitats and ecosystems in China. Moreover, primary productivity was ranked among the top ecological factors for seven heterotrophic and mixotrophic species, and nitrate concentration was ranked among the top ecological factors for four autotrophic species, thus indicating an increase in the risk of changes in HSA with boosted primary productivity and aggravated eutrophication in the China seas and adjacent waters.

Greater than 70%–80% of species would suffer a decrease in HSA and northward migration in the near term and at the end of the century. This may result in the emergence of new types of HABs in the northern area of the China seas and exert great impacts on biodiversity and adaptability in the future. Global climate change poses a serious challenge to China, and efforts should be made to encourage further research to examine the future biogeographical impacts of toxin-producing species and develop countermeasures for the environmental management of coastal habitats and ecosystems.

Acknowledgements

We would like to thank Editage (www.editage.cn) for English language editing.

References

Assis J, Tyberghein L, Bosch S, et al. 2018. Bio-ORACLE v2.0: Extending marine data layers for bioclimatic modelling. Global Ecology and Biogeography, 27(3): 277–284, doi: 10.1111/geb.12693

Beaumont C D. 1981. Regression diagnostics—Identifying influential data and sources of collinearity. Journal of the Operational Research Society, 32(2): 157–158

Bertram J, Newman E A, Dewar R C. 2019. Comparison of two maximum entropy models highlights the metabolic structure of metacommunities as a key determinant of local community assembly. Ecological Modelling, 407: 108720, doi: 10.1016/j.ecolmodel.2019.108720

Burkholder J M, Glibert P M, Skelton H M. 2008. Mixotrophy, a major mode of nutrition for harmful algal species in eutrophic waters. Harmful Algae, 8(1): 77–93, doi: 10.1016/j.hal.2008.08.010

Cai Rongshuo, Han Zhiqiang, Yang Zhengxian. 2020. Impacts and risks of changing ocean on marine ecosystems and dependent communities and related responses. Climate Change Research (in Chinese), 16(2): 182–193

Cai Rongshuo, Tan Hongjian, Guo Haixia. 2019. Responses and compound risks of the coastal China areas to global change. Journal of Applied Oceanography (in Chinese), 38(4): 514–527

Chen Baohong, Wang Kang, Lin Hui. 2019. *Akashiwo sanguinea* blooms in Chinese waters in 1998–2017. Marine Pollution Bulletin, 149: 110652, doi: 10.1016/j.marpolbul.2019.110652

China National Marine Science Data Center. 2021. Further analysis of global monthly average data (in Chinese). http://mds.nmdis.org.cn/[2019-08-06/2021-05-16]

Elith J, Phillips S J, Hastie T, et al. 2011. A statistical explanation of MaxEnt for ecologists. Diversity and Distributions, 17(1): 43–57, doi: 10.1111/j.1472-4642.2010.00725.x

Gu Haifeng. 2011. Morphology, phylogenetic position, and ecophysiology of *Alexandrium ostenfeldii* (Dinophyceae) from the Bohai Sea, China. Journal of Systematics and Evolution, 49(6): 606–616, doi: 10.1111/j.1759-6831.2011.00160.x

Gu Haifeng, Liu Tingting, Vale P, et al. 2013. Morphology, phylogeny and toxin profiles of *Gymnodinium inusitatum* sp. nov., *Gymnodinium catenatum* and *Gymnodinium microreticulatum* (Dinophyceae) from the Yellow Sea, China. Harmful Algae, 28: 97–107

Gu Haifeng, Wu Yiran, Lü Songhui, et al. 2022. Emerging harmful algal bloom species over the last four decades in China. Harmful Algae, 111: 102059, doi: 10.1016/j.hal.2021.102059

Guo Hao, Ding Dewei, Lin Feng'ao, et al. 2015. Characteristics and patterns of red tide in China coastal waters during the last 20 a. Advances in Marine Science (in Chinese), 33(4): 547–558

Guo Hao, Lin Feng'ao, Liu Yongjian, et al. 2014. High-incidence HABs causative species in China coastal waters and the forewarning method based on the HABs risk index. Marine Environmental Science (in Chinese), 33(1): 94–98

IPCC. 2013. Summary for policymakers. In: Climate Change 2013: The Physical Science Basis. Contribution of Working Group Ⅰ to the Fifth Assessment Report of the Intergovernmental Panel on Climate Change. Cambridge, United Kingdom and New York, NY, USA: Cambridge University Press, 3–29

IPCC. 2019. Summary for policymakers. In: Climate Change and Land: An IPCC Special Report on Climate Change, Desertification, Land Degradation, Sustainable Land Management, Food Security, and Greenhouse Gas Fluxes in Terrestrial Ecosystems. Cambridge, United Kingdom and New York, NY, USA: Cambridge University Press, 3–34

IPCC. 2021. Summary for policymakers. In: Climate Change 2021: The Physical Science Basis. Contribution of Working Group Ito the Sixth Assessment Report of the Intergovernmental Panel on Climate Change. Cambridge, United Kingdom and New York, NY, USA: Cambridge University Press, 3–32

Kariya T, Kurata H, Hayashi T. 2024. A modelling framework for regression with collinearity. Journal of Statistical Planning and Inference, 228: 95–115, doi: 10.1016/j.jspi.2023.07.001

Li Xueding. 2021. Occurrence characteristics of the red tide in Fujian coastal waters during the last two decades. Marine Environmental Science (in Chinese), 40(4): 601–610

Li Jiangyue, Chang Hong, Liu Tong, et al. 2019. The potential geographical distribution of *Haloxylon* across Central Asia under climate change in the 21st century. Agricultural and Forest Meteorology, 275: 243–254, doi: 10.1016/j.agrformet.2019.05.027

Lin Senjie, Ji Nanjing, Luo Hao. 2019. Recent progress in marine harmful algal bloom research. Oceanologia et Limnologia Sinica (in Chinese), 50(3): 495–510

Liu Guiying, Ge Kun, Song Lun, et al. 2015. The research trend of *Karenia mikimotoi*. Marine Sciences (in Chinese), 39(9): 117–122

Lü Songhui, Cen Jingyi, Wang Jianyan, et al. 2019. The research status quo, hazard, and ecological mechanisms of *Karenia mikimotoi* red tide in coastal waters of China. Oceanologia et Limnologia Sinica (in Chinese), 50(3): 487–494

Melo-Merino S M, Reyes-Bonilla H, Lira-Noriega A. 2020. Ecological niche models and species distribution models in marine environments: A literature review and spatial analysis of evidence. Ecological Modelling, 415: 108837, doi: 10.1016/j.ecolmodel.2019.108837

Merow C, Smith M J, Silander J A. 2013. A practical guide to MaxEnt for modeling species' distributions: what it does, and why inputs and settings matter. Ecography, 36(10): 1058–1069, doi: 10.1111/j.1600-0587.2013.07872.x

Meshgi B, Majidi-Rad M, Hanafi-Bojd A A, et al. 2019. Ecological niche modeling for predicting the habitat suitability of fascioliasis based on maximum entropy model in southern Caspian Sea littoral, Iran. Acta Tropica, 198: 105079, doi: 10.1016/j.actatropica.2019.105079

Ministry of Natural Resources of the People's Republic of China. 1998–2022. Bulletin of China Marine Disaster (1998–2022) (in Chinese). https://www.mnr.gov.cn/sj/sjfw/hy/gbgg/zghyzhgb/index_1.html[2023-12-13/2023-04-08]

Phillips S J, Anderson R P, Dudík M, et al. 2017. Opening the black box: An open-source release of MaxEnt. Ecography, 40(7): 887–893, doi: 10.1111/ecog.03049

Phillips S J, Anderson R P, Schapire R E. 2006. Maximum entropy modeling of species geographic distributions. Ecological Modelling, 190(3–4): 231–259, doi: 10.1016/j.ecolmodel.2005.03.026

Phillips S J, Dudík M. 2008. Modeling of species distributions with MaxEnt: New extensions and a comprehensive evaluation. Ecography, 31(2): 161–175, doi: 10.1111/j.0906-7590.2008.5203.x

Phillips S J, Dudík M, Schapire R E. 2004. A maximum entropy approach to species distribution modeling. In: Proceedings of the Twenty-First International Conference on Machine Learning. Banff, Alberta, Canada: ACM, 83

Qi Yuzao, Zou Jingzhong, Liang Song. 2003. Red Tide along the Coast of China (in Chinese). Beijing: Science Press, 1–2

Shen Yongping, Wang Guoya. 2013. Key findings and assessment results of IPCC WGI Fifth Assessment Report. Journal of Glaciology and Geocryology (in Chinese), 35(5): 1068–1076

Soofi E S. 2000. Principal information theoretic approaches. Journal of the American Statistical Association, 95(452): 1349–1353, doi: 10.1080/01621459.2000.10474346

Tillmann U, Elbrächter M, Krock B, et al. 2009. *Azadinium spinosum* gen. et sp. nov. (Dinophyceae) identified as a primary producer of azaspiracid toxins. European Journal of Phycology, 44(1): 63–79, doi: 10.1080/09670260802578534

Tyberghein L, Verbruggen H, Pauly K, et al. 2012. Bio-ORACLE: A global environmental dataset for marine species distribution modelling. Global Ecology and Biogeography, 21(2): 272–281, doi: 10.1111/j.1466-8238.2011.00656.x

Wang Rulin, Li Qing, Feng Chuanhong, et al. 2017. Predicting potential ecological distribution of *Locusta migratoria tibetensis* in China using MaxEnt ecological niche modeling. Acta Ecologica Sinica (in Chinese), 37(24): 8556–8566

Wang Changyou, Wang Xiulin, Liang Shengkang, et al. 2010. The methods for calibrating average concentration in the domain and estimating average annual concentration of pollutants in the sea area being partially or totally different from target domains. Haiyang Xuebao (in Chinese), 32(2): 155–160

Wang Changyou, Xu Yiwen, Gu Haifeng, et al. 2023a. Expansion risk of the toxic dinoflagellate *Gymnodinium catenatum* blooms in

Chinese waters under climate change. Ecological Informatics, 75: 102042, doi: 10.1016/j.ecoinf.2023.102042

Wang Changyou, Xu Yiwen, Gu Haifeng, et al. 2024. Potential geographical distribution of harmful algal blooms caused by the toxic dinoflagellate *Karenia mikimotoi* in the China Sea. Science of the Total Environment, 906: 167741, doi: 10.1016/j.scitotenv.2023.167741

Wang Endong, Zhang Lianjun, Chen Hong, et al. 2023b. Collinearity-oriented sensitivity analysis for patterning energy factor significance in buildings. Journal of Building Engineering, 73: 106685, doi: 10.1016/j.jobe.2023.106685

Wang Zhaohui, Zhang Yuning, Wang Wenting, et al. 2022. Distribution of dinoflagellate cysts in surface sediments on the Dongshan Bay, Fujian Province, China. Journal of Tropical Oceanography (in Chinese), 41(4): 154–162

Xie Pengfei, Gu Yanbin, Sui Weina, et al. 2019. Big data challenges for species distribution models in predicting potential distribution of marine species. Marine Information (in Chinese), 34(1): 51–61

Xu Yixiao, He Xilin, Lee Wai Hin, et al. 2021. Ciguatoxin-producing dinoflagellate *Gambierdiscus* in the Beibu Gulf: First report of toxic *Gambierdiscus* in Chinese Waters. Toxins (Basel), 13(9): 643, doi: 10.3390/toxins13090643

Yan Huyong, Feng Lei, Zhao Yufei, et al. 2020. Predicting the potential distribution of an invasive species, *Erigeron canadensis L.*, in China with a maximum entropy model. Global Ecology and Conservation, 21: e00822

Yu Zhiming, Chen Nansheng. 2019. Emerging trends in red tide and major research progresses. Oceanologia et Limnologia Sinica (in Chinese), 50(3): 474–486

Zhang Qingtian. 2013. Review on the annual variation of red tides in China Sea. Environmental Monitoring in China (in Chinese), 29(5): 98–102

Zhang Danhua, Hu Yuanman, Liu Miao. 2019. Potential distribution of *Spartinal alterniflora* in China coastal areas based on MaxEnt niche model. Chinese Journal of Applied Ecology (in Chinese), 30(7): 2329–2337

Zhou Jian, Wang Wei, Wu Zhihong, et al. 2020. The basic characteristics and prevention countermeasures of red tide in Shandong coast waters. Marine Environmental Science (in Chinese), 39(4): 537–543

Supplementary information:

Fig. S1. Potential distribution area of harmful dinoflagellate under RCP26 scenario in 2050.

Fig. S2. Potential distribution area of harmful dinoflagellate under RCP26 scenario in 2100.

Fig. S3. Potential distribution area of harmful dinoflagellate under RCP85 scenario in 2050.

Fig. S4. Potential distribution area of harmful dinoflagellate under RCP85 scenario in 2100.

The supplementary information is available online at https://doi.org/10.1007/s13131-024-2451-3 and http://www.aosocean.com/. The supplementary information is published as submitted, without typesetting or editing. The responsibility for scientific accuracy and content remains entirely with the authors.